JBIC Journal of Biological Inorganic Chemistry (2023) 28:101–115
https://doi.org/10.1007/s00775-022-01974-z

ORIGINAL PAPER

Insights into the role of the cobalt(III)-thiosemicarbazone complex as a potential inhibitor of the Chikungunya virus nsP4

Daniel Oliveira Silva Martins[1,2] · Rafael Aparecido Carvalho Souza[3] · Marjorie Caroline Liberato Cavalcanti Freire[4] · Nathalya Cristina de Moraes Roso Mesquita[4] · Igor Andrade Santos[1] · Débora Moraes de Oliveira[1] · Nilson Nicolau Junior[5] · Raphael Enoque Ferraz de Paiva[6] · Mark Harris[7] · Carolina Gonçalves Oliveira[3] · Glaucius Oliva[4] · Ana Carolina Gomes Jardim[1,2]

Received: 26 May 2022 / Accepted: 19 October 2022 / Published online: 9 December 2022

Abstract

Chikungunya virus (CHIKV) is the causative agent of chikungunya fever, a disease that can result in disability. Until now, there is no antiviral treatment against CHIKV, demonstrating that there is a need for development of new drugs. Studies have shown that thiosemicarbazones and their metal complexes possess biological activities, and their synthesis is simple, clean, versatile, and results in high yields. Here, we evaluated the mechanism of action (MOA) of a cobalt(III) thiosemicarbazone complex named $[Co^{III}(L^1)_2]Cl$ based on its in vitro potent antiviral activity against CHIKV previously evaluated (80% of inhibition on replication). Furthermore, the complex has no toxicity in healthy cells, as confirmed by infecting BHK-21 cells with CHIKV-*nanoluciferase* in the presence of the compound, showing that $[Co^{III}(L^1)_2]Cl$ inhibited CHIKV infection with the selective index of 3.26. $[Co^{III}(L^1)_2]Cl$ presented a post-entry effect on viral replication, emphasized by the strong interaction of $[Co^{III}(L^1)_2]Cl$ with CHIKV non-structural protein 4 (nsP4) in the microscale thermophoresis assay, suggesting a potential mode of action of this compound against CHIKV. Moreover, in silico analyses by molecular docking demonstrated potential interaction of $[Co^{III}(L^1)_2]Cl$ with nsP4 through hydrogen bonds, hydrophobic and electrostatic interactions. The evaluation of ADME-Tox properties showed that $[Co^{III}(L^1)_2]Cl$ presents appropriate lipophilicity, good human intestinal absorption, and has no toxicological effect as irritant, mutagenic, reproductive, and tumorigenic side effects.

✉ Carolina Gonçalves Oliveira
carolina@ufu.br

✉ Ana Carolina Gomes Jardim
jardim@ufu.br

1 Institute of Biomedical Sciences, Federal University of Uberlândia, Avenida Amazonas, 4C- Room 216, Umuarama, Uberlândia, MG 38405-302, Brazil

2 São Paulo State University, IBILCE, São José do Rio Preto, SP, Brazil

3 Bioinorganic Chemistry Group, Institute of Chemistry, Federal University of Uberlândia, Uberlândia, MG 38408-100, Brazil

4 Physics Institute of São Carlos, University of São Paulo, São Carlos, SP, Brazil

5 Molecular Modeling Laboratory, Institute of Biotechnology, Federal University of Uberlândia, Uberlândia, Brazil

6 Department of Fundamental Chemistry, Institute of Chemistry, University of São Paulo, São Paulo, SP, Brazil

7 Faculty of Biological Sciences and Astbury Centre for Structural Molecular Biology, University of Leeds, Leeds, UK

Graphical abstract

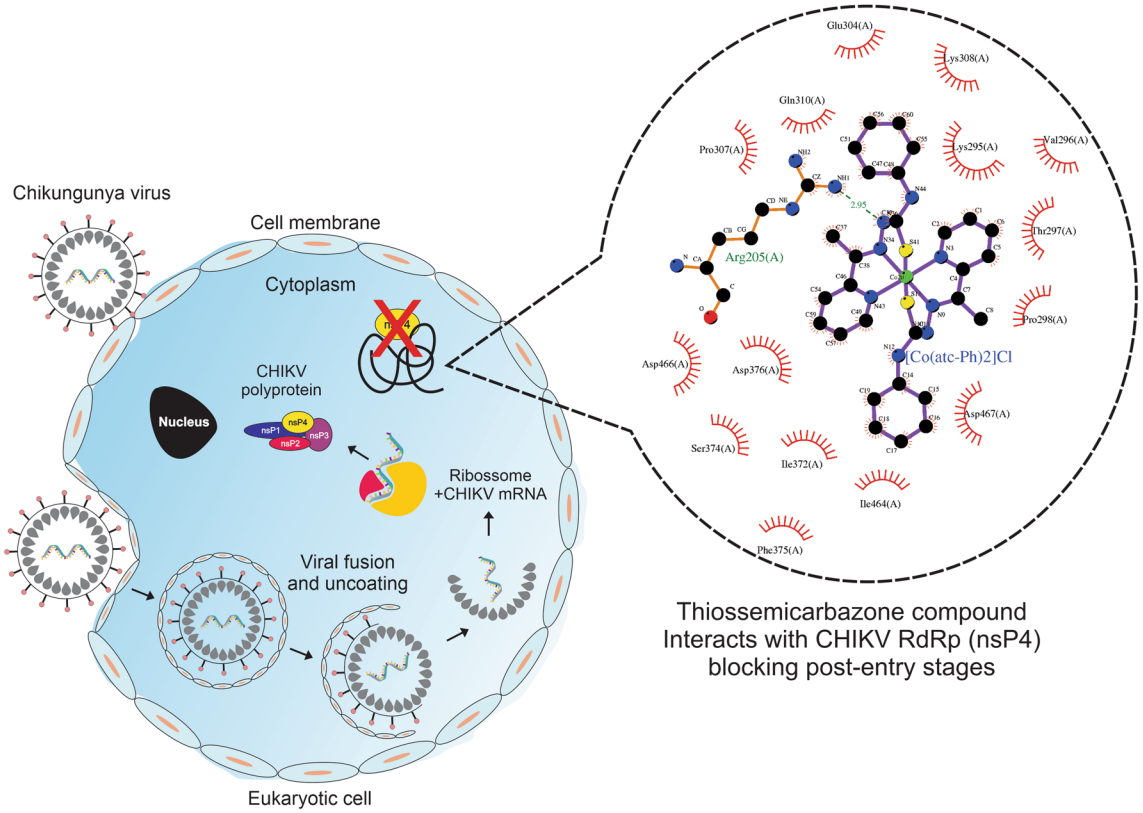

Keywords Metal ion · Antiviral activity · Chikungunya virus · Mechanism of action · Molecular docking · ADME-Tox

Introduction

The chikungunya virus (CHIKV) is the etiological agent of chikungunya fever, a tropical disease characterized by high fever, rash, joint pain, and arthralgia [1]. The virus is transmitted through the bite of *Aedes* mosquitoes and the infection caused by CHIKV can progress to a disabling chronic disease or may cause neurological complications such as Guillain–Barre syndrome [2, 3].

CHIKV is an alphavirus that belongs to the family *Togaviridae* (ICTV, 2019). It is an enveloped virus of icosahedral capsid and a positive-sense single-strand RNA of approximately 12 kb [4]. CHIKV genome contains two open reading frames (ORFs) [4]. The 5' ORF encodes four non-structural proteins (nsP1–nsP4) and the 3' ORF is transcribed into a subgenomic RNA which is translated into five structural proteins (C, E1, E2, E3, and 6 K) [5, 6]. The non-structural proteins play substantial roles in the virus replication forming a replicase complex [7], nsP4 being defined as the CHIKV RNA-dependent RNA polymerase (RdRp). In this way, CHIKV replication is directly dependent on nsP4 activity that represents a promising target for antiviral therapeutic [8]. Therefore, disruption or inactivity of the nsP4 activity can result in the impairment of the CHIKV replicative cycle, decreasing virus replication and also impacting in the clinical progress of Chikungunya fever.

CHIKV was first isolated in Tanzania in 1952 and, for a while, cases related to CHIKV occurred in the Southeast Asian regions, Africa, and Oceania [9]. In 2006, an outbreak was documented in some Indian Ocean islands [10] and, a year later, France and Italy reported cases of this infection [11, 12]. In 2013, an outbreak occurred in Central America, in the Caribbean Islands [13, 14]. Then, the virus spread through North and South America [15]. In Brazil, according to the Urban Arboviruses Monitoring Report, 132,205 cases of chikungunya fever were registered in 2019, with an incidence rate of 62.9 cases/per 100,000 inhabitants in 2019. Northeast and Southeast were the regions with the highest incidence rates in the Country, with 104.6 and 59.4 cases/100,000 inhabitants, respectively. In the same year, 92 deaths were confirmed by CHIKV infection, and a higher lethality rate was observed in elderly people over 60 [16]. In 2020, during the outbreak of COVID-19, the Brazilian states of Bahia, Mato Grosso, Espirito Santo, and Rio de Janeiro

showed an increase in likely cases of chikungunya, according to the bulletin released by the surveillance secretary [17]. Furthermore, according to CDC (Centers for Disease Control), over 110 countries reported CHIKV infection cases until October 2020 [18].

Currently, there is no licensed treatment against CHIKV showing the need for new molecules that possess antiviral activity [19]. The treatment of infected patients is palliative and aims to relieve the symptoms caused by the infection. According to the World Health Organization (WHO), the most appropriate drug is acetaminophen 1 g 3–4 times per day for adults, and 50–60 mg per kg per day for children [20]. Other non-steroidal analgesics are also recommended, except aspirin which can cause platelet dysfunction [21].

Thiosemicarbazones (TSCs) are a class of synthetic compounds known to have versatile chemistry, low costs of production, and few atoms waste (only molecules of water are usually released during synthesis reactions) [22]. Teitz and coworkers (1994) described the antiviral activity of *N*-methylisatin-β4′:4′-diethylthiosemicarbazone, a compound that demonstrated to disrupt the synthesis of Human Immunodeficiency Virus (HIV) structural proteins. TSCs derivatives have also demonstrated antiviral activity described against herpes simplex virus (HSV), affecting the expression of structural proteins of HSV, suppressing capsid assembly, and inhibiting cell-to-cell spread [23].

Besides that, TSCs are also recognized as excellent metal binders, therefore, being widely explored as ligands in coordination chemistry. It also provides very stable and high-quality chelating organometallics [24–26]. Interestingly, TSCs metal complexes have demonstrated antimicrobial [27], antiprotozoal [28], and anticancer [29], and antiviral activities [30]. Usually, thiosemicarbazones are coordinated with metals such as Copper(II) and cobalt(III). These metals are present in the human organism, therefore, representing pre-existing biological pathways that will regulate their therapeutic levels. For example, cobalt(III) is an essential trace element in the human body and also is a necessary component of vitamin B_{12} [31]. Physiological speciation involving these endogenous metal ions can increase the bioavailability of these compounds, decrease the cytotoxicity and even improve their biological activity [32].

Considering our previous findings on the antibacterial action and preliminary anti-CHIKV activities of the complexes of the type $[Co^{III}(atc–R)_2]Cl$ (R = methyl, Me or phenyl, Ph), as well as the free ligands [33], here we further characterized the anti-CHIKV activity of the cobalt(III) coordination compound with the thiosemicarbazone ligand $[Co^{III}(L^1)_2]Cl$ (Fig. 1) and exploited its potential mode of action. Our data show that cobalt(III)-conjugated thiosemicarbazones may provide an interesting source of compounds for the development of future antivirals to treat chikungunya fever.

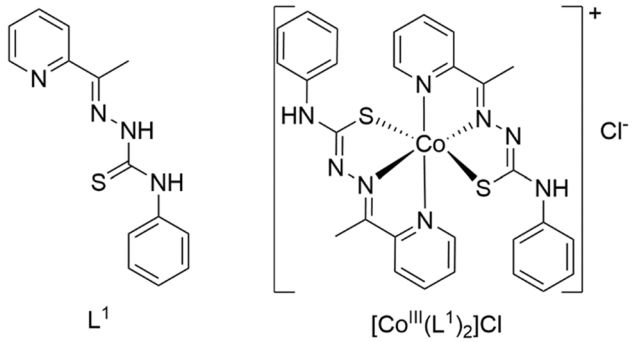

Fig. 1 Chemical structure of the TSC free ligand L^1 and its cobalt(III) complex $[Co^{III}(L^1)_2]Cl$

Materials and methods

Preparation of the compounds

The compounds studied here were previously synthesized and characterized as described by Fernandes and coworkers [34]. L^1 was prepared by refluxing 4-phenyl-3-thiosemicarbazide and 2-acetylpyridine (1:1) in ethanolic solutions [35]. Briefly, the reaction of $CoCl_2$•$6H_2O$ and L^1 (1:2) in ethanol (15 mL) provided $[Co^{III}(L^1)_2]Cl$ (Fig. 1). The products were characterized and purities evaluated [33, 34]. The characterization of the compounds was previously certified by techniques such as 1H and 13C NMR, high-resolution mass spectrometry, LC–MS/MS and fragmentation study, and previously reported [34]. The compounds were dissolved in dimethyl sulfoxide (DMSO) and stored at − 20 °C for the biological assays. Dilutions of the compounds in a complete medium were made immediately prior to the experiments to reach a maximum final concentration of 0.1% DMSO. For all the assays performed, cells were treated with DMSO 0.1% as untreated control.

Cell culture

BHK-21 cells (fibroblasts derived from Syrian golden hamster kidney; ATCC® CCL-10™), which are susceptible to CHIKV infection [36], were maintained in Dulbecco's modified Eagle's medium (DMEM; Sigma-Aldrich) supplemented with 100U/mL of penicillin (Hyclone Laboratories, USA), 100 mg/mL of streptomycin (Hyclone Laboratories, USA), 1% of non-essential amino acids (Hyclone Laboratories, USA) and 1% of fetal bovine serum (FBS, Hyclone Laboratoires, USA) in a humidified 5% CO_2 incubator at 37 °C.

Rescue of CHIKV-*nanoluc* reporter virus

The CHIKV expressing *nanoluciferase* reporter (CHIKV-*nanoluc*) used for the antiviral assays were designed from a CHIKV sequence based on CHIKV isolate LR2006OPY1 (East/Central/South African genotype). The cDNA plasmid of CMV-CHIKV-*nanoluc* contains a CMV promoter, SV40 terminator, and a sequence encoding *nanoluciferase* protein inserted into the region encoding the C-terminal domain of viral nsP3 protein [37, 38]. The production of CHIKV-*nanoluc* virions was carried out as previously described [39–41]. Briefly, 2.3×10^7 BHK-21 cells seeded in a cell culture flask were transfected with 1.5 µg of CMV-CHIKV-*nanoluc* plasmid, using lipofectamine 3000® and Opti-Mem medium to rescue CHIKV *nanoluc* reporter virus. Forty-eight hours post-transfection, the supernatant was collected and stored at − 80 °C.

To determine the viral titer, 5×10^5 BHK-21 cells were seeded in each of 6 wells plate 24 h prior to the infection. Then, the cells were infected with tenfold serially diluted supernatant of CHIKV *nanoluc* for 1 h at 37 °C. The inoculum was removed, and the cells were washed with phosphate-buffered saline (PBS) to remove the unbound virus and added of cell culture media supplemented with 1% penicillin, 1% streptomycin, 2% FBS and 1% carboxymethyl cellulose (CMC). Infected cells were incubated for 2 days in a humidified 5% CO_2 incubator at 37 °C, followed by fixation with 3% formaldehyde and stained with 0.5% violet crystal and the viral foci were counted to determine CHIKV-*nanoluc* titers [42].

Cell viability through MTT assay

Cell viability was measured by MTT [3-(4,5-dimethylthiazol-2-yl)-2,5-diphenyl tetrazolium bromide] (Sigma–Aldrich) assay. BHK-21 cells were cultured in 96 well plate and treated with concentrations of each compound for 16 h at 37 °C with 5% of CO_2. Twenty-four hours post-treatment, compound-containing media was removed and MTT solution at 1 mg/mL was added to each well, incubated for 1 h, and replaced with 100 µL of DMSO to solubilize the formazan crystals. The absorbance was measured at 560 nm on Glomax microplate reader (Promega, USA). Cell viability was calculated according to the equation $(T/C) \times 100\%$, in which T and C represented the optical density of the treated well and control groups, respectively. DMSO was used as untreated control. The cytotoxic concentration of 50% (CC_{50}) was calculated using GraphPad Prism 8 (Graph Pad Software).

Antiviral activity assays

BHK-21 cells were seeded at a density of 5×10^4 cells per well into 48-well plates 24 h prior to the infection. CHIKV-*nanoluc* [38, 41] at a multiplicity of infection (M.O.I) of 0.01 and compounds at the non-cytotoxicity concentration were simultaneously added to cells. Samples were harvested in Renilla luciferase lysis buffer (Promega, USA) at 16 h post-infection (h.p.i.) and virus replication levels were quantified by measuring *nanoluciferase* activity using the Renilla luciferase Assay System (Promega, USA). The effective concentration of 50% inhibition (EC_{50}) was calculated using GraphPad Prism 8. The values of CC_{50} and EC_{50} were used to calculate the selectivity index ($SI = CC_{50}/EC_{50}$).

To evaluate the protective activity of the compound, cells were pre-treated for 1 h with 50 µM of $[Co^{III}(L^1)_2]Cl$, extensively washed with PBS to remove the compound, and infected with CHIKV-*nanoluc* (M.O.I. of 0.01). The effect of $[Co^{III}(L^1)_2]Cl$ on early stages of infection was analyzed by incubating the virus and compound simultaneously with BHK-21 cells for 1 h. Then, the compound was removed, and cells were added of fresh medium. Additionally, to investigate the activity of the compound in the post-entry stages of the viral replicative cycle, cells were infected with CHIKV for 1 h, washed extensively with PBS to remove the unabsorbed virus, and added of compound-containing media. Luminescence levels were measured 16 h.p.i. to analyze the virus replication rates.

Intercalation assay

To investigate whether the compound interacts with the double-stranded RNA (dsRNA), an experiment using the previously described protocol [43, 44] was performed. Briefly, fifteen nanograms of the dsRNA were incubated with 50 µM of $[Co^{III}(L^1)_2]Cl$ at room temperature for 45 min and electrophoresed on a 1% agarose gel prior to analysis by densitometry. DMSO and Doxorubicin (DOX) at 100 µM were used as the untreated and positive control, respectively.

CHIKV nsP4 cloning, overexpression, and purification

The coding region of chikungunya non-structural protein 4 (nsP4) (GenBank KP164572.1; PROT-ID AJY53709.1) was cloned into pET-SUMO expression vector, generating the nsP4_pET-SUMO/LIC expression vector. Rosetta (DE3) *E. coli* (Novagen) cells were transformed with nsP4_pET-M11/LIC and grown in TB (Terrific Broth) medium, supplemented with 50 µg ml^{-1} kanamycin and 34 µg ml^{-1} chloramphenicol at 37 °C. The cell growth was monitored until reaching the optical density (OD_{600nm}) of 1.0. The protein expression was induced by adding 1 mM of Isopropyl

β-D-1-thiogalactopyranoside (IPTG), at 18 °C and maintained for 16 h. Cells were harvested by centrifugation and cell pellets were resuspended in lysis buffer (50 mM Tris pH 8.0, 500 mM NaCl, and 10% glycerol). Cells were lysed by sonication and cell debris was separated by centrifugation.

The nsP4 was purified using an AKTA Purifier System (GE Healthcare). The first purification step was affinity chromatography using a HisTrap HP 5.0 ml column (GE Healthcare) and the elution was performed using 250 mM imidazole. Concomitantly, the buffer was exchanged through dialysis and the His-tag-SUMO was cleavaged by TEV protease overnight at 4 °C. Another affinity chromatography step was performed using the same system to collect the protein after cleavage. The protein was concentrated, and a final purification step was done through size-exclusion chromatography on an XK 26/1000 Superdex 75 column (GE Healthcare) pre-equilibrated in buffer 50 mM Tris pH 8.0, 200 mM NaCl and 5% glycerol. The final protein sample was analyzed by SDS-PAGE electrophoresis to confirm its purity. The concentration was determined spectrophotometrically in a Nanodrop 1000 spectrophotometer.

MicroScale thermophoresis (MST)

Experiments were performed on a Monolith® NT.115 instrument (Nanotemper technologies). The nsP4 was labeled on cysteine residues with NT-647-Maleimide dye (Nanotemper Technologies) using the Monolith NTTM Protein Labeling Kit RED-MALEIMIDE as per the manufacturer's instructions. The cys-labeled nsP4 was used to perform MicroScale Thermophoresis experiments, at the final concentration of 25 nM. An initial binding test was carried out with compound $[Co^{III}(L^1)_2]Cl$ at the concentration of 500 µM, to check the interaction between the protein and the compound. The assay control was performed using cys-labeled nsP4 with 5% DMSO. Then, a serial dilution of the $[Co^{III}(L^1)_2]Cl$ from 500 to 0.015 µM (15 nM) was performed to obtain the binding curve. The dissociation constant (K_d) was obtained by fitting the binding curve with the Hill function, using GraphPad Prism 8 (Graph Pad Software).

Molecular docking analysis

The 3D structure of $[Co^{III}(L^1)_2]Cl$ was obtained by DFT at the pbe0/def2-tzvp [45] level of theory using ORCA 4.2.0 [46, 47]. Auxiliary basis sets AuxJ (def2/J) [48] and AuxC (def2-svp/C) [49] were also used. Optimized structures were rendered using Chemcraft (graphical software for visualization of quantum chemistry computations, https://www.chemcraftprog.com). A representative sequence of nsP4 extracted from the viral polyprotein (UniProt id: Q8JUX6) was modeled using the RoseTTAFold [50] on the Rosetta online server (https://robetta.bakerlab.org/). The nsP4 tridimensional model was assessed using ERRAT [51], Ramachandran Plot [52], and Verify 3D [53] tools in the SAVES v6.0 server (https://saves.mbi.ucla.edu/). The nsP4 binding site was predicted using COACH [54] based on the RoseTTAFold-predicted structure. COACH is a meta-server approach that combines multiple function annotation results to generate ligand binding site predictions. COACH results indicate a binding site similar to the site where the Uridine 5′-Triphosphate (UTP) interacts with the crystal structure of HCV ns5B polymerase (PDBid: 4RY5). Thus, $[Co^{III}(L^1)_2]Cl$ was docked with the modeled protein using GOLD [55]. GOLD performs a search for the best interacting pose of the chosen molecule in the receptor binding site using a genetic algorithm (GA) and the scoring function ChemPL. The binding site was defined by the UTP position based on the 4RY5 structure and extrapolated to the modeled nsP4. The GA parameters were set to the default values for the run, with M-L bonds treated as zero-order bonds. The poses generated are then ranked and the solution with the best score was chosen. The intramolecular interactions in the best-ranked pose were analyzed using DS Visualizer (BIOVIA, Dassault Systèmes, Discovery Studio Visualizer, v 20.1, San Diego: Dassault Systèmes, 2020).

ADME-Tox predictions

The free online platforms SwissADME (www.swissadme.ch) and OSIRIS Property Explorer® (http://www.cheminfo.org/Chemistry/Cheminformatics/Property_explorer/index.html) were used to evaluate the parameters of absorption, distribution, metabolism, excretion, and toxicity (ADME-Tox).

Statistical analysis

Individual experiments were performed in triplicate and in a minimum of three times to confirm the reproducibility of the results. Differences between means of readings were compared using analysis of variance (one-way or two-way ANOVA) or Student's *t*-test using GraphPad Prism 8 (Graph Pad Software). P values ≤ 0.05 were considered to be statistically significant.

Results and discussion

CHIKV is an emerging arbovirus with a high impact on public health in tropical and non-tropical areas. In recent years, outbreaks have occurred around the world affecting many patients with chikungunya fever, the disease caused by CHIKV [2, 56, 57]. Currently, there is no antiviral therapy against CHIKV, demonstrating the need to identify new anti-CHIKV compounds [19].

In this context, thiosemicarbazones (TSCs) have previously been demonstrated to possess antiviral activity against HIV and HSV by disrupting the synthesis of structural proteins and also capsid assembly [23, 25]. Additionally, TSCs are described as possessing interesting motifs for metal binders and thus being coordinated with metals such as copper(II) and cobalt(III) [58, 59]. Cobalt(III) is an endogenous metal, and therefore, the bioavailability of cobalt(III)-like compounds can be increased, as well as their biological properties, in therapeutic protocols for human diseases [31, 60]. Considering the chemical versatility of the synthesis of TSC and the biological properties of cobalt(III)-like compounds, we previously analyzed complexes of the type $[Co^{III}(atc–R)_2]Cl$ which demonstrated interesting antibacterial and antiviral activities [33]. Here, we characterized the anti-CHIKV activity of the $[Co^{III}(L^1)_2]Cl$, a Cobalt(III) coordination compound with the thiosemicarbazone ligand with promising antiviral proprieties.

$[Co^{III}(L^1)_2]Cl$ inhibits CHIKV infection in vitro

We previously demonstrated that the treatment of CHIKV-infected cells with the cobalt(III)-conjugated thiosemicarbazone $[Co^{III}(L^1)_2]Cl$ (Fig. 1) reduced CHIKV infection, and cell viability was not affected compared to the treatment with its organic ligand [33]. In this work, $[Co^{III}(L^1)_2]Cl$ had its antiviral activity characterized using a recombinant CHIKV engineered to express the *nanoluciferase* reporter (CHIKV-*nanoluc*) (Fig. 2A). To assess the effect of $[Co^{III}(L^1)_2]Cl$ on cell viability and virus infection, we performed a dose–response assay to determine the effective concentration of 50% (EC_{50}) and the cytotoxicity concentration of 50% (CC_{50}) values for this complex. BHK-21 cells were infected with CHIKV-*nanoluc* and treated with $[Co^{III}(L^1)_2]Cl$ at concentrations ranging from 0.14 to 300 µM, and viral replication levels were evaluated by measuring the nanoluciferase reporter activity at 16 h.p.i. (Fig. 2B). Employing this range of concentrations, it was determined that the $[Co^{III}(L^1)_2]Cl$ has an EC_{50} of 19 µM, CC_{50} of 62 µM, and SI of 3.26 (Fig. 2B). For further analysis, cells were treated with $[Co^{III}(L^1)_2]Cl$ at 50 µM, which significantly inhibited 94% of the CHIKV infection (cell viability > 80%) (Fig. 2C).

Our results showed that $[Co^{III}(L^1)_2]Cl$ significantly reduced virus post-entry to host cells at non-toxic concentrations, and therefore, the effect of this complex was further evaluated. As shown by other authors, and in agreement with our results, TSCs had their antiviral activity previously described against HIV and HSV, in a post-entry manner. The authors suggested that the mechanism of action for these compounds was related to the disruption of the synthesis of the structural protein and also capsid assembly [23, 25]. Additionally, Langsjoen et al. showed that the gold salt auranofin displayed antiviral activity against CHIKV with

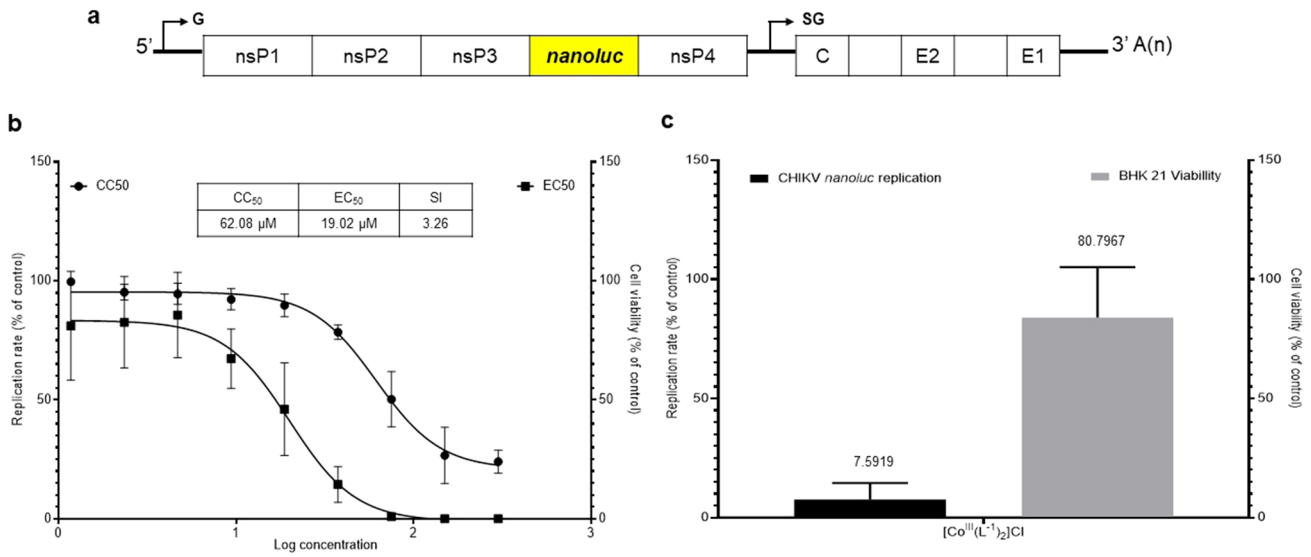

Fig. 2 **A** Schematic representation of the engineered Chikungunya virus *nanoluciferase* genome (CHIKV-*nanoluc*). **B** The effective concentration (EC_{50}) and cytotoxic concentration (CC_{50}) of $[Co^{III}(L^1)_2]Cl$. BHK-21 cells were treated with increasing concentrations of $[Co^{III}(L^1)_2]Cl$ ranging from 0.14 to 300 µM. CHIKV replication was measured by *nanoluciferase* activity (indicated by ■) and cellular viability was measured using an MTT assay (indicated by ●). Mean values of three independent experiments each measured in quadruple including the standard deviation are shown. **C** BHK-21 cells were infected with CHIKV-*nanoluc* and simultaneously treated with $[Co^{III}(L^1)_2]Cl$ at 50 µM for 16 h. After treatment, cells were lysed and *nanoluciferase* levels were measured to assess the CHIKV replication rate. An MTT assay was carried out in parallel. Mean values of a minimum of three independent experiments each measured in triplicate are represented

a Therapeutic Index (TI) of 104.5 12 h.p.i, aiming to target oxidative folding pathways [61].

$[Co^{III}(L^1)_2]Cl$ is a post-entry inhibitor of the CHIKV replicative cycle

To analyze the effects of $[Co^{III}(L^1)_2]Cl$ on different stages of the CHIKV replicative cycle, viruses and compounds were added to BHK-21 cells at different times. First, cells were pre-treated with $[Co^{III}(L^1)_2]Cl$ for 1 h, washed to remove the compound, and were infected with CHIKV-*nanoluc* (Fig. 3A). To assess the effect on the early stages of infection, CHIKV-*nanoluc* and $[Co^{III}(L^1)_2]Cl$ were simultaneously added to the BHK-21 cells for 1 h, followed by repeated cell washes to remove the inoculum and addition of fresh media (Fig. 3B). To investigate the interference with post-entry steps of infection, cells were first infected with CHIKV-*nanoluc*, washed to remove the unbounded virus, and then a media-containing compound was added (Fig. 3C). The results obtained from all these experimental conditions demonstrated that $[Co^{III}(L^1)_2]Cl$ at 50 µM inhibited up to 94% of the CHIKV post-entry replication step (Fig. 3C) but had no effect on the early stages of the replicative cycle (Fig. 3B) or in protecting cells from infection (Fig. 3A).

Despite being widely studied as antifungal [62], antibacterial [63], and largely exploited in cancer therapy [64], metal complexes are not studied nearly as much as antiviral agents in comparison to other applications such as anticancer [65], and only a few studies have reported the antiviral activity of cobalt(III) complexes [66]. In the latest 1990, a cobalt chelate series (CTC) (General formula [Co(acacen)(L)2]$^+$) of cobalt(III) complexes were studied as antiviral molecules against Herpes Simplex I virus (HSV-I) in vitro. The drug Doxovir™ (also named Co-1 or CTC-96 in the literature) significantly inhibited HSV-I infectivity in Vero cells at 5 µg mL^{-1} [67]. In the earlies 2000, Schwartz and coworkers reported that Co-1 at 50 µg mL^{-1} inhibited the early stages of HSV-1 infection in Vero cells, impairing virus penetration in the initial fusion stage between cell and virus. They have also found that this compound inhibited Varicella-zoster virus (VZV) plaque formation [68]. The antiviral activity of Co-1 was also described against Human Adenovirus type 5 (Ad5) in cell culture, acting as a virucidal compound, and also in rabbit model [69].

Another cobalt complex, the CTC compound Co-sb, showed to inhibit HIV-1 in vitro by Louie and Meade, by disrupting zinc finger structures, inhibiting transcription factors, and also interactions of some viral proteins with zinc fingers domains [70]. Moreover, the cobalt(III) complex sodium hydrogen butylimino bis-8,8-[5-(3-oxa-pentoxy)-3-cobalt bis(1,2-dicarbollide)]di-ate([$Co(NH_2C(NH)$-$NHC(NH)NH^sBu)_3]^3+$) showed antiviral activity against HIV-I, inhibiting HIV-I protease interactions in the hydrophobic sites of the protein, with EC_{50} 0.25 µM in PM-1 cells [71, 72]. This compounds also showed antiviral activity against H1N1 virus, reducing H1N1 cytopathic effect in MDCK cells, with EC_{50} of 125 µg/mL and SI of 8 [73].

What is more, there are only two research articles reporting cobalt(III) complexes as antiviral agents against arboviruses: Miranda and coworkers described the activity of

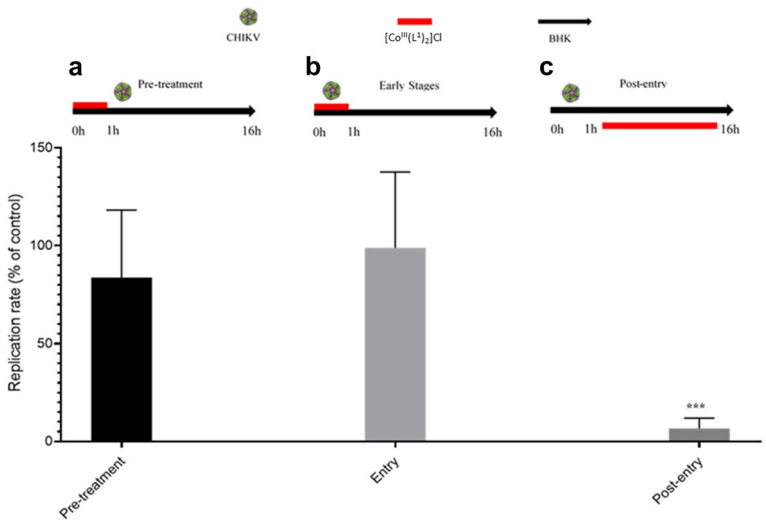

Fig. 3 $[Co^{III}(L^1)_2]Cl$ impairs post-entry stages of the CHIKV replicative cycle. **A** BHK-21 cells were pre-treated with $[Co^{III}(L^1)_2]Cl$ for 1 h, washed to completely remove the compounds, and were infected with CHIKV-*nanoluc*. **B** BHK-21 cells were infected with CHIKV-*nanoluc* and simultaneously treated with $[Co^{III}(L^1)_2]Cl$ 50 µM for 1 h. Then, cells were washed to remove the virus and compound and were replaced with fresh media. **C** BHK-21 cells were infected with CHIKV- *nanoluc* for 1 h, washed to remove unbound virus and added fresh media-containing compound. For all protocols, *nanoluciferase* activity levels were measured 16 h.p.i. Mean values of a minimum of three independent experiments each measured in triplicate are represented. ***$P < 0.01$ were considered significant

this class of metal complexes against Dengue virus (DENV) and Yellow fever virus (YFV) [73]; and our previous data published on CHIKV [33]. The compounds investigated by Miranda and coworkers were the cobalt(III) complex of protoporphyrin IX (CoPPIX) and tinprotoporphyrinIX (SnPPIX) [74]. For DENV-2, DENV-3 and YFV CoPPIX presented EC_{50} of 3.91, 0.77 and 3.74 μmol l^{-1} in HepG2 cells, while SnPPIX presented 3.26, 0.85 and 0.37 μmol l^{-1}. For DENV, the compounds seem to disrupt or impair protein synthesis, and block virus adsorption and penetration in BHK 21 cells, with the same MOA that inhibited YFV.

Further compounds (non-metals) were reported with antiviral activity against post-entry stages of CHIKV replicative cycle. For example, the guanosine analog Ribavirin, described as a substrate of RdRp of HCV [75, 76], disrupted CHIKV replication with EC_{50} of 3.41 μM in Vero cells, 2 days post-infection [77]. Additionally, the 6-azauridine, an uridine analog used to treat psoriasis, also impaired CHIKV replication by disrupting CHIKV RNA replication. Briolant and coworkers showed that this compound possesses SI of 204 in Vero cells, 8.5 times higher than ribavirin used in the same study as a positive control [78].

Insights on mechanisms of action of $[Co^{III}(L^1)_2]Cl$

Based on the activity of the complex on CHIKV post-entry stages, we investigated whether this compound could interact with the viral dsRNA. During the chikungunya replicative cycle, a double-strand RNA (dsRNA) is formed as replicative intermediate molecules. Considering that some compounds possess antiviral activity by intercalating into this dsRNA [43] and that many metal complexes are DNA intercalators [79, 80] or DNA binders [81], we assessed the dsRNA interaction capabilities of $[Co^{III}(L^1)_2]Cl$ by agarose gel electrophoresis. $[Co^{III}(L^1)_2]Cl$ was incubated with 15 nM of dsRNA and analyzed in an agarose gel. Doxorubicin (DOX) at 100 μM and DMSO 0.1% were used as positive and untreated controls, respectively. Since $[Co^{III}(L^1)_2]Cl$ had no intercalation activity, ethidium bromide was able to intercalate to the dsRNA and the band was visualized as observed in the untreated control (Fig. 4). Densitometry analysis confirmed that the cobalt(III) conjugated compound did not intercalate with dsRNA (Fig. 4).

Aiming to access initial information about a possible target for $[Co^{III}(L^1)_2]Cl$ action, the CHIKV nsP4 was synthesized and purified in vitro (Fig. 5A). Thereby, the interaction between nsP4 and $[Co^{III}(L^1)_2]Cl$ was evaluated by Microscale Thermophoresis (MST). The binding affinity curve was obtained using a serial dilution of the compound to obtain information on the dissociation constant (k_d). The results demonstrated that the binding affinity curve presented well-defined bound and unbound states, suggesting the occurrence of interaction between the CHIKV nsP4 and the $[Co^{III}(L^1)_2]Cl$ (Fig. 5B). Through the obtained curve, the estimated $k_d \pm \Delta k_d$ for this interaction was 8.35 ± 0.681 μM.

To achieve evidence on the mechanism of action of this compound, we performed a dsRNA interaction assay. During the CHIKV replication cycle, a dsRNA is formed as a replicative intermediate molecule during the synthesis of a negative sense sRNA which is a template for the next viral replication stages. Considering that some compounds that acted on post-entry stages of virus replicative cycle demonstrated antiviral activity intercalating in dsRNA species [43], we investigated the interference of $[Co^{III}(L^1)_2]Cl$ with a dsRNA, however, $[Co^{III}(L^1)_2]Cl$ seems to not act by this mechanism.

Knowing that replication is a very important process in the virus replication cycle, we investigated the interaction

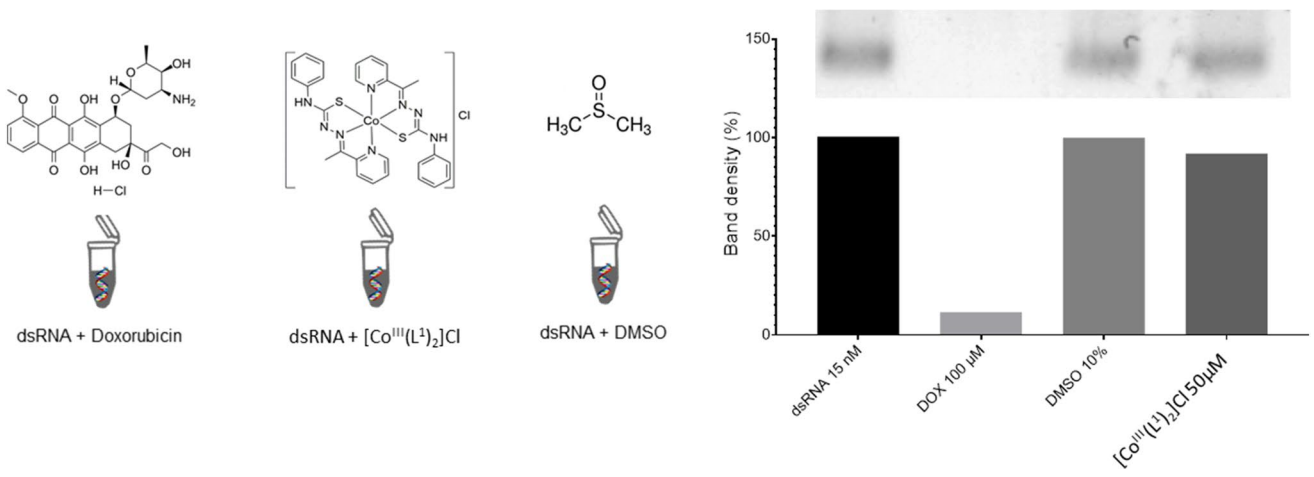

Fig. 4 $[Co^{III}(L^1)_2]Cl$ does not intercalate intro dsRNA. $[Co^{III}(L^1)_2]Cl$ was incubated with 15 nM of dsRNA for 45 min and submitted to electrophoresis using a 1% agarose gel (run in 1 × TAE buffer) stained with ethidium bromide, followed by densitometry analysis. DMSO 0.1% and Doxorubicin (DOX) at 100 μM were used as untreated and positive controls, respectively

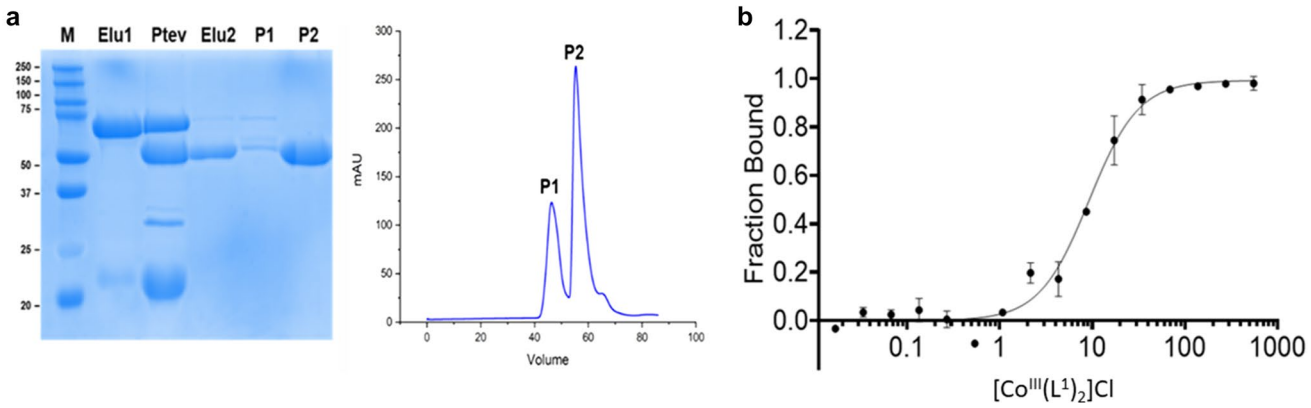

Fig. 5 $[Co^{III}(L^1)_2]Cl$ interacts with CHIKV nsP4. **A** SDS-PAGE Electrophoresis gel of nsP4 purification. M: Molecular weight marker; Elu1: Elution of His-tag-SUMO-nsP4 (approximately 70 kDa) by affinity chromatography step; Ptev: sample after incubation with TEV protease, indicating the cleavage of His-tag-SUMO; Elu2: Elution of nsP4 (54.54 kDa) after TEV protease cleavage; The P1 and P2 refer to the two peaks in the chromatogram (right) of the gel filtration step, corresponding to the eluted fractions. The purified nsP4 was eluted in P2 (54.54 kDa). **B** Binding affinity curve of nsP4 and $[Co^{III}(L^1)_2]Cl$, obtained by Microscale Thermophoresis experiments. Estimated $kd \pm \Delta kd = 8.35 \pm 0.681$ µM

of $[Co^{III}(L^1)_2]Cl$ with the non-structural protein 4 (nsP4), a nsP which plays an essential role in the replicative complex activity. The nsP4 is an RNA-dependent RNA polymerase (RdRp) responsible for the synthesis of new RNA strands that will be incorporated into the viral progeny resulting from the replicative cycle. As it is crucial for viral replication, the RdRp has been an important target for antiviral therapies. Studies have shown compounds with antiviral activity against CHIKV replication, but only a few were documented suggesting nsP4 as a target. Some examples include benzimidazole [82], hesperetin-A derivates [83], and favipiravir [84]. The availability of only a few studies for nsP4 can be explained due to the lack of structural information about this protein, such as the absence of an experimentally solved three-dimensional structure of CHIKV nsP4, which limits studies on the search for specific inhibitors based on this target.

Thus, to investigate whether this protein could be a possible target for $[Co^{III}(L^1)_2]Cl$, we cloned, overexpressed, and purified CHIKV nsP4, and interaction studies were carried out by MicroScale Thermophoresis with different concentrations of the compound. Our data show that $[Co^{III}(L^1)_2]Cl$ interacted with CHIKV nsP4, suggesting that it might be a potential mechanism of antiviral action of this complex. Furthermore, molecular docking analysis suggested that the compound potentially interacts with CHIKV nsP4 through hydrogen bonding and electrostatic interactions in the Uridine 5'-Triphosphate (UTP) binding site, and probably impairing the initiation and elongation of new viral RNA, corroborating with the in vitro results.

Molecular docking analysis

In view of CHIKV nsP4 as a possible target for $[Co^{III}(L^1)_2]Cl$ complex, molecular docking was performed for a better understanding of the nature of the interactions between this protein and the compound. To this end, a prediction of the nsP4 protein structure was performed using the RoseTTA-Fold method and the structure was validated using Verify 3D, ERRAT, and Ramachandran Plot formalism (Supplementary Figs. 1–3). The 3D structure of $[Co^{III}(L^1)_2]Cl$ was obtained by DFT (Fig. 6A). The compound $[Co^{III}(L^1)_2]Cl$ was then submitted as a ligand for molecular docking analysis using the nsP4 protein model as a receptor. The COACH software suggested the Uridine 5'-Triphosphate (UTP) binding site as the probable spot for the $[Co^{III}(L^1)_2]Cl$ interaction. The best scored pose (ChemPL = 66.92) was selected (Fig. 6B). Analyzing the intramolecular interactions, it can be observed a hydrogen bond involving the N–H group of Arg205 amino acid (2.95 Å). Furthermore, hydrophobic interactions with Pro298 and Lys295 amino acids (4.95 Å and 4.11 Å, respectively) were predicted, along with aromatic-sulfur interaction with Cys506 amino acid (5.30 Å). Finally, van der Waals interactions were observed with Pro307, Gln310, Glu304, Lys308, Val296, Thr297, Asp467, Ile464, Phe375, Ile372, Ser374, Asp376, and Asp466 (Fig. 7A and B).

ADME-Tox predictions

The evaluation of ADME-Tox properties of L^1 and $[Co^{III}(L^1)_2]Cl$ complex was carried out to verify the

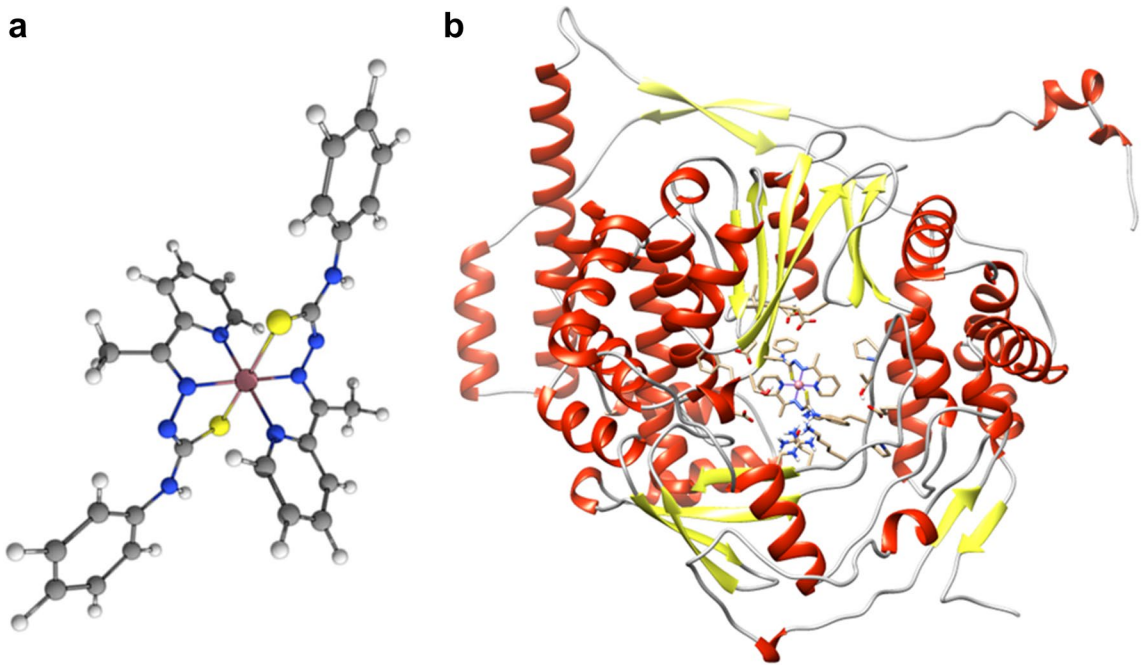

Fig. 6 Prediction of $[Co^{III}(L^1)_2]Cl$ and CHIKV NSP4 structures. **A** DFT-optimized structure of compound $[Co^{III}(L^1)_2]Cl$ at the pbe0/def2-tvp level of theory as implemented in ORCA 4.2.0. Color code: white—hydrogen; gray—carbon; blue—nitrogen; yellow—sulfur; light pink—cobalt. **B** The predicted nsP4 structure interacting with $[Co^{III}(L^1)_2]Cl$

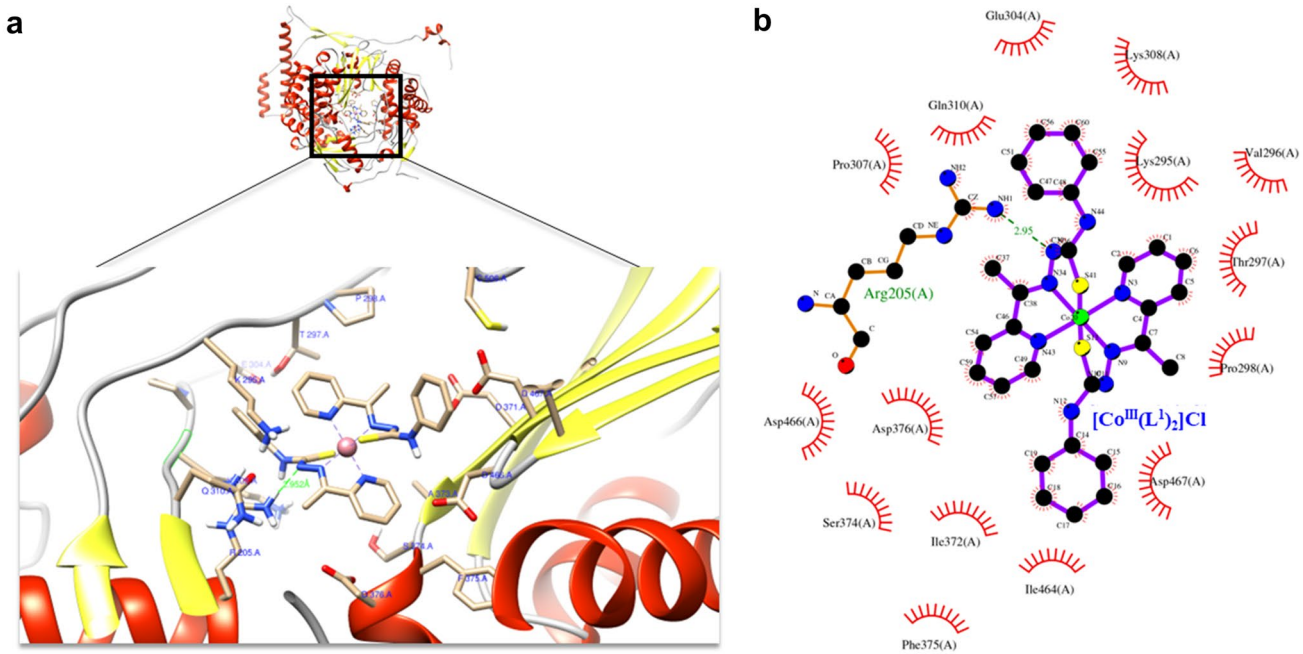

Fig. 7 In silico analysis of potential interactions between $[Co^{III}(L^1)_2]Cl$ and CHIKV NSP4. **A** Best ranked pose obtained by the molecular docking of $[Co^{III}(L^1)_2]Cl$ (represented in red) into the CHIKV nsP4 model. **B** CHIKV NSP4 and $[Co^{III}(L^1)_2]Cl$ atomic interactions. Green dashed line indicates hydrogen bond, magenta, and light magenta dashed lines indicate hydrophobic interactions, yellow dashed lines indicate electrostatic interactions, orange dashed lines indicate pi-sulfur interactions, and numbers in black indicate the interaction distances in angstroms (Å)

physicochemical properties as lipophilicity, water-solubility, human intestinal absorption (HIA), blood–brain barrier penetration (BBB), inhibition of isoenzymes belonging to the CYP450 system and toxicological effect (irritant, mutagenic, reproductive and tumorigenic). The results are shown in Tables 1 and 2.

According to the results listed in Table 1, the L^1 is in according to Lipinski's rules while $[Co^{III}(L^1)_2]Cl$ complex breaks one of Lipinski's rules because of its higher molecular weight (MW > 500). Other important parameters are Log S, MR, and TPSA concerning to hydrophobicity of a given compound, and, consequently, the ability to cross plasmatic membranes and permeate cells. Those parameters provide information about the absorption and distribution of a drug in the organism [85]. According to the results shown in Table 1, the L^1 and $[Co^{III}(L^1)_2]Cl$ complex could show good lipophilicity and the ability to cross plasmatic membranes. Although this is an initial study, these results reveal that $[Co^{III}(L^1)_2]Cl$ has the potential to be used as a metal drug. Furthermore, these data may be useful for future studies in the case of evaluating the absorption and biodistribution of this complex and its analogs in vivo.

The L^1 and $[Co^{III}(L^1)_2]Cl$ complex were also evaluated for human intestinal absorption (HIA), blood–brain barrier penetration (BBB), and inhibition of isoenzymes belonging to the CYP450 system as a preliminary theoretical study (Table 2). The results showed that both candidates had high absorption in the intestine, none of the compounds were able to cross the blood–brain barrier as well as none inhibited the CYP2D6 and CYP3A4 isoenzymes belonging to the CYP450 system. Furthermore, the toxicological effects (irritant, mutagenic, carcinogenic, and tumorigenic) were also evaluated. In general, the L^1 has higher toxic effects than the $[Co^{III}(L^1)_2]Cl$ complex, which demonstrates the importance of complexation with a trace metal and shows that the introduction of the metal cobalt ion reduces the toxic effects of the free ligand [86].

Although the complex presents some unsatisfactory results as a potential to be carcinogenic and does not follow all the rules of Lipinsk, it still represents a candidate to the development of antiviral drugs. Some drugs used to treat diseases also violate specific rules and continue to be used as medications, such as ivermectin, tenofovir dis-oproxil fumarate (TDF), ceftadizime, and isoniazid. Acarbose, Chloroquine, Lopinavir, Amodiaquine are predicted by the web server Admetsar 2.0 as hepatotoxic and mutagenic [87].

Table 1 In silico evaluation of Lipinski parameters of L^1 and $[Co^{III}(L^1)_2]Cl$ complex

Parameters	L^1	$[Co^{III}(L^1)_2]Cl$
Physicochemical properties		
Formula	$C_{14}H_{14}N_4S$	$C_{30}H_{30}N_8S_2ClCo$
MW[a]	270.35 g/mol	661.13 g/mol
Num. rotatable bonds	5	6
Num. H–bonds acceptors	2	2
Num. H–bonds donors	2	2
MR[b]	81.92	191.87
TPSA[c]	81.40 Å^2	133.96 Å^2
Lipophilicity		
log $P_{o/w}$ [d,e]	2.49	2.16
Water solubility		
log *S*	–3.44	–9.07
Class[f]	Soluble	Poorly soluble
Druglikeness		
Lipinski[g]	Yes	No: MW > 500
Bioavailability score	0.55	0.55

[a]MW: Molecular Weight

[b]MR: Molar Refractivity

[c]TPSA: Topological Polar Surface Area

[d]Consensus log $P_{o/w}$ = Average of all five predictions

[e]log $P_{o/w}$ = partition coefficient between *n*-octanol/water

[f]Class = Ali classes: insoluble < –10 < poor < –6 < moderately soluble < –4 < soluble < –2 < very soluble < 0 < highly

[g]Lipinski = MW ≤ 500; log $P_{o/w}$ ≤ 5; H–bond donors ≤ 5; H–bond acceptors ≤ 10

Conclusion

In summary, we have shown that the $[Co^{III}(L^1)_2]Cl$ inhibits the post-entry stage of CHIKV infection, potentially by interacting and interfering with the nsP4 activity. Due to the lack of studies with CHIKV nsP4, there is no positive control for in vitro assays, and also, there is no well-established structure yet. Therefore, we suggest that $[Co^{III}(L^1)_2]Cl$ might interact with nsP4 and interferes with its activity, however, we acknowledge that interpretation of these experiments is challenging and further studies are necessary.

Table 2 Data on the main pharmacokinetic and toxicology properties of L^1 and $[Co^{III}(L^1)_2]Cl$ complex

Compound	HIA	BBB penetration	CYP3A4 inhibitor	CYP2D6 inhibitor	Reproductive	Mutagenic	Tumorigenic	Irritant
L^1	High	No	No	No	High	High	Low	Low
$[Co^{III}(L^1)_2]Cl$	High	No	No	No	Low	Median	Low	Low

It is also important to emphasize the broad antimicrobial activities of this compound since it has already shown activity against *Mycobacterium tuberculosis* [34], *E. faecalis*, *S. salivarius*, *S. sanguinis*, *S. mitis*, *S. mutans,* and *L. paracasei* [33]. In this way, this compound could be applied for the treatment of multiple diseases caused by such bacteria and the chikungunya virus, which can be interesting for the pharmaceutical industry and generate great social impact. Although metallodrugs are widely exploited in cancer treatment, some antimicrobials and skin diseases, there is no metallodrug licensed to treat any virus infection. Herein we presented data about the antiviral activity and suggest potential MOA of $[Co^{III}(L^1)_2]Cl$ against chikungunya, thus reinforcing the relevance of these results to the current state of antiviral research and the potential of this class of metal complexes as a proposed therapeutic molecule candidate to be further explored.

It is worth to mention that there are only a few published works using Cobalt(III) coordinated compounds as therapeutic molecules, highlighting the relevance to the published data exploring such combination. From a vast bibliography, with several papers exploring this coordination, we can then make a better scientific judgment whether the application of these complexes is worthwhile or not for in vivo and clinical trials, reinforcing the application of these data for the research landscape of therapeutic targets against chikungunya fever.

The conclusions obtained from molecular docking studies demonstrated a significant binding of the complex with CHIKV NSP4 structures which is consistent with the in vitro antiviral activity. Furthermore, the antiviral activity of $[Co^{III}(L^1)_2]Cl$ against other viruses which impact human health may be the target of future investigation. Considering the pivotal role of RdRp in *Alphavirus* replication, our results may contribute to future studies on inhibitors of nsP4, representing a relevant contribution to the field of antiviral research against CHIKV. The significant antiviral profile together with ADME-Tox results provides an interesting approach for future in vivo studies.

Supplementary Information The online version contains supplementary material available at https://doi.org/10.1007/s00775-022-01974-z.

Acknowledgements We thank Andres Merits (Institute of Technology, University of Tartu, Tartu, Estonia) for the provision of the CHIKV expressing-nanoluciferase reporter. The authors received financial support from the Royal Society—Newton Advanced Fellowship (grant reference NA 150195 to ACGJ and MH), FAPEMIG (Minas Gerais Research Foundation APQ-02872-16, APQ-01164-22 and APQ-01487-22), from the Wellcome Trust (Investigator Award—grant reference 096670 to MH), and CAPES—Finance Code 001. ACGJ is grateful to Coordenação de Aperfeiçoamento de Pessoal de Nível Superior (CAPES)—Brasil—Prevention and Combat of Outbreaks, Endemics, Epidemics and Pandemics—Finance Code #88881.506794/2020-01. REFP thanks the Sao Paulo Research Foundation (FAPESP), grant #2018/21537-6. IAS received a PhD scholarship (# 142495/2020-4) from the CNPq (National Councel of Technological and Scientific Development).

Data availability All data generated or analyzed during this study are included in this published article and, its supplementary information files.

Declarations

Conflict of interest The authors declare that the research was conducted in the absence of any commercial or financial relationships that could be construed as a potential conflict of interest.

References

1. Gould E, Pettersson J, Higgs S et al (2017) Emerging arboviruses: Why today? One Heal (Amsterdam, Netherlands) 4:1–13. https://doi.org/10.1016/j.onehlt.2017.06.001
2. Paixão ES, Rodrigues LC, da Costa MCN et al (2018) Chikungunya chronic disease: a systematic review and meta-analysis. Trans R Soc Trop Med Hyg 112:301–316. https://doi.org/10.1093/trstmh/try063
3. Stegmann-Planchard S, Gallian P, Tressières B et al (2019) Chikungunya, a risk factor for Guillain-Barré syndrome. Clin Infect Dis. https://doi.org/10.1093/cid/ciz625
4. Khan AH, Morita K, del Carmen PM et al (2002) Complete nucleotide sequence of chikungunya virus and evidence for an internal polyadenylation site. J Gen Virol 83:3075–3084. https://doi.org/10.1099/0022-1317-83-12-3075
5. Kumar S, Mamidi P, Kumar A et al (2015) Development of novel antibodies against non-structural proteins nsP1, nsP3 and nsP4 of chikungunya virus: potential use in basic research. Arch Virol 160:2749–2761. https://doi.org/10.1007/s00705-015-2564-2
6. Voss JE, Vaney M-C, Duquerroy S et al (2010) Glycoprotein organization of Chikungunya virus particles revealed by X-ray crystallography. Nature 468:709–712. https://doi.org/10.1038/nature09555
7. Rausalu K, Utt A, Quirin T et al (2016) Chikungunya virus infectivity, RNA replication and non-structural polyprotein processing depend on the nsP2 protease's active site cysteine residue. Sci Rep. https://doi.org/10.1038/srep37124
8. Ahola T, Merits A (2016) Functions of Chikungunya virus nonstructural proteins. Chikungunya virus. Springer International Publishing, Cham, pp 75–98
9. Ross RW (1956) The virus: isolation, pathogenic properties and relationship to the epidemic. The Newala Epidemic. https://doi.org/10.1017/S0022172400044442
10. Schuffenecker I, Iteman I, Michault A et al (2006) Genome microevolution of chikungunya viruses causing the Indian Ocean outbreak. PLoS Med 3:1058–1070. https://doi.org/10.1371/journal.pmed.0030263
11. Grandadam M, Caro V, Plumet S et al (2011) Chikungunya virus, Southeastern France. Emerg Infect Dis 17:910–913. https://doi.org/10.3201/eid1705.101873
12. Rezza G, Nicoletti L, Angelini R et al (2007) Infection with chikungunya virus in Italy: an outbreak in a temperate region. Lancet 370:1840–1846. https://doi.org/10.1016/S0140-6736(07)61779-6
13. Yactayo S, Staples JE, Millot V et al (2016) Epidemiology of Chikungunya in the Americas. J Infect Dis 214:S441–S445. https://doi.org/10.1093/infdis/jiw390
14. Mowatt L, Jackson ST (2014) Chikungunya in the Caribbean: an epidemic in the making. Infect Dis Ther 3:63–68. https://doi.org/10.1007/s40121-014-0043-9

15. Vega-Rua A, Zouache K, Girod R et al (2014) High level of vector competence of *Aedes aegypti* and *Aedes albopictus* from ten American countries as a crucial factor in the spread of Chikungunya virus. J Virol 88:6294–6306. https://doi.org/10.1128/JVI.00370-14
16. da Saúde M, de Saúde em V (2020) Boletim Epidemiológico - Monitoramento dos casos de arboviroses urbanas transmitidas pelo Aedes Aegypti (dnegue, chikungunya e zika), Semanas epidemiológicas 1 a 52. Bol Epidemiológico Arboviroses 51:1–13
17. da Saúde M, de Saúde em V (2020) Boletim Epidemiológico - Monitoramento dos casos de arboviroses urbanas transmitidas pelo Aedes Aegypti (dnegue, chikungunya e zika), Semanas epidemiológicas 1 a 14, 2020. Bol Epidemiológico Arboviroses 51:1–13
18. CDC (2019) Countries and territories where chikungunya cases have been reported. Centers Dis Control Prev 1
19. Dey D, Siddiqui SI, Mamidi P et al (2019) The effect of amantadine on an ion channel protein from Chikungunya virus. PLoS Negl Trop Dis 13:e0007548. https://doi.org/10.1371/journal.pntd.0007548
20. WHO (2008) Guidelines on Clinical Management of Chikungunya Fever. World Heal Organ
21. Panning M, Grywna K, van Esbroeck M et al (2008) Chikungunya Fever in Travelers Returning to Europe from the Indian Ocean Region, 2006. Emerg Infect Dis 14:416–422. https://doi.org/10.3201/eid1403.070906
22. Du X, Guo C, Hansell E et al (2002) Synthesis and Structure−Activity Relationship Study of Potent Trypanocidal Thio Semicarbazone Inhibitors of the Trypanosomal Cysteine Protease Cruzain. J Med Chem 45:2695–2707. https://doi.org/10.1021/jm010459j
23. Genova P, Varadinova T, Matesanz AI et al (2004) Toxic effects of bis(thiosemicarbazone) compounds and its palladium(II) complexes on herpes simplex virus growth. Toxicol Appl Pharmacol 197:107–112. https://doi.org/10.1016/j.taap.2004.02.006
24. Antonini I, Claudi F, Cristalli G et al (1981) N*-N*-S* Tridentate ligand system as potential antitumor agents. J Med Chem 24:1181–1184. https://doi.org/10.1021/jm00142a012
25. Casas JS, García-Tasende MS, Sordo J (2000) Main group metal complexes of semicarbazones and thiosemicarbazones. A structural review. Coord Chem Rev 209:197–261. https://doi.org/10.1016/S0010-8545(00)00363-5
26. Oliveira CG, Romero-Canelón I, Silva MM et al (2019) Palladium(<scp>ii</scp>) complexes with thiosemicarbazones derived from pyrene as topoisomerase IB inhibitors. Dalt Trans 48:16509–16517. https://doi.org/10.1039/C9DT02570G
27. Kasuga NC, Sekino K, Ishikawa M et al (2003) Synthesis, structural characterization and antimicrobial activities of 12 zinc(II) complexes with four thiosemicarbazone and two semicarbazone ligands. J Inorg Biochem 96:298–310. https://doi.org/10.1016/S0162-0134(03)00156-9
28. Bharti N, Husain K, Gonzalez GM et al (2002) Synthesis and in vitro antiprotozoal activity of 5-nitrothiophene-2-carboxaldehyde thiosemicarbazone derivatives. Bioorg Med Chem Lett 12:3475–3478. https://doi.org/10.1016/S0960-894X(02)00703-5
29. Oliveira CG, Romero-Canelón I, Coverdale JPC et al (2020) Novel tetranuclear Pd II and Pt II anticancer complexes derived from pyrene thiosemicarbazones. Dalt Trans 49:9595–9604. https://doi.org/10.1039/D0DT01133A
30. Teitz Y, Ronen D, Vansover A et al (1994) Inhibition of human immunodeficiency virus by N-methylisatin-β4′:4′-diethylthiosemicarbazone and N-allylisatin-β-4′:4′-diallythiosemicarbazone. Antiviral Res 24:305–314. https://doi.org/10.1016/0166-3542(94)90077-9
31. Czarnek K, Terpiłowska S, Siwicki AK (2015) Review paper Selected aspects of the action of cobalt ions in the human body. Cent Eur J Immunol 2:236–242. https://doi.org/10.5114/ceji.2015.52837
32. West DX, Liberta AE, Padhye SB et al (1993) Thiosemicarbazone complexes of copper(II): structural and biological studies. Coord Chem Rev 123:49–71. https://doi.org/10.1016/0010-8545(93)85052-6
33. de Fernandes LP, Silva JMB, Martins DOS et al (2020) Fragmentation study, dual anti-bactericidal and anti-viral effects and molecular docking of Cobalt(III) complexes. Int J Mol Sci 21:8355. https://doi.org/10.3390/ijms21218355
34. Oliveira CG, da Maia PIS, Miyata M et al (2014) Cobalt(III) complexes with thiosemicarbazones as potential anti- mycobacterium tuberculosis agents. J Braz Chem Soc. https://doi.org/10.5935/0103-5053.20140149
35. Richardson DR, Kalinowski DS, Richardson V et al (2009) 2-acetylpyridine thiosemicarbazones are potent iron chelators and antiproliferative agents: redox activity, iron complexation and characterization of their antitumor activity. J Med Chem 52:1459–1470. https://doi.org/10.1021/jm801585u
36. Davis JL, Hodge HM, Campbell WE (1971) Growth of chikungunya virus in baby hamster kidney cell (BHK-21-clone 13) suspension cultures. Appl Microbiol 21:338–341
37. Pohjala L, Utt A, Varjak M et al (2011) Inhibitors of alphavirus entry and replication identified with a stable chikungunya replicon cell line and virus-based assays. PLoS ONE 6:e28923. https://doi.org/10.1371/journal.pone.0028923
38. Matkovic R, Bernard E, Fontanel S et al (2018) The host DHX9 DExH-box helicase is recruited to chikungunya virus replication complexes for optimal genomic RNA translation. J Virol 93:1–17. https://doi.org/10.1128/JVI.01764-18
39. de Oliveira DM, de Santos IA, Martins DOS et al (2020) Organometallic complex strongly impairs chikungunya virus entry to the host cells. Front Microbiol. https://doi.org/10.3389/fmicb.2020.608924
40. dos Pereira AKS, Santos IA, da Silva WW et al (2021) Memantine hydrochloride: a drug to be repurposed against Chikungunya virus? Pharmacol Reports. https://doi.org/10.1007/s43440-021-00216-4
41. Santos IA, Shimizu JF, de Oliveira DM et al (2021) Chikungunya virus entry is strongly inhibited by phospholipase A2 isolated from the venom of Crotalus durissus terrificus. Sci Rep 11:8717. https://doi.org/10.1038/s41598-021-88039-4
42. Baer A, Kehn-Hall K (2014) Viral concentration determination through plaque assays: using traditional and novel overlay systems. J Vis Exp. https://doi.org/10.3791/52065
43. Campos GRF, Bittar C, Jardim ACG et al (2017) Hepatitis C virus in vitro replication is efficiently inhibited by acridone Fac4. J Gen Virol 98:1693–1701. https://doi.org/10.1099/jgv.0.000808
44. Santos IA, dos Pereira AK, S, Guevara-Vega M, et al (2022) Repurposing potential of rimantadine hydrochloride and development of a promising platinum(II)-rimantadine metallodrug for the treatment of Chikungunya virus infection. Acta Trop 227:106300. https://doi.org/10.1016/j.actatropica.2021.106300
45. Weigend F, Ahlrichs R, Peterson KA et al (2005) Balanced basis sets of split valence, triple zeta valence and quadruple zeta valence quality for H to Rn: design and assessment of accuracy. Phys Chem Chem Phys 7:3297. https://doi.org/10.1039/b508541a
46. Neese F (2012) The ORCA program system. Wiley Interdiscip Rev Comput Mol Sci 2:73–78. https://doi.org/10.1002/wcms.81
47. Neese F (2018) Software update: the ORCA program system, version 4.0. WIREs Comput Mol Sci 8:e1327. https://doi.org/10.1002/wcms.1327
48. Weigend F (2006) Accurate Coulomb-fitting basis sets for H to Rn. Phys Chem Chem Phys 8:1057–1065. https://doi.org/10.1039/b515623h

49. Hellweg A, Hättig C, Höfener S, Klopper W (2007) Optimized accurate auxiliary basis sets for RI-MP2 and RI-CC2 calculations for the atoms Rb to Rn. Theor Chem Acc 117:587–597. https://doi.org/10.1007/s00214-007-0250-5
50. Minkyung B, Frank D, Ivan A et al (2021) Accurate prediction of protein structures and interactions using a three-track neural network. Science (80-) 373:871–876. https://doi.org/10.1126/science.abj8754
51. Colovos C (1993) Verification of protein structures: patterns of nonbonded atomic interactions. Mol Biol 2:1511–1519
52. Laskowski RA, Macarthur MW, Moss DS, Thornton JM (1993) PROCHECK: a program to check the stereochemical quality of protein structures. J Appl Cryst 26:283–291
53. Eisenberg D, Lüthy R, Bowie JU (1997) VERIFY3D: assessment of protein models with three-dimensional profiles. Methods Enzymol 277:396–404. https://doi.org/10.1016/S0076-6879(97)77022-8
54. Yang J, Roy A, Zhang Y (2013) Protein-ligand binding site recognition using complementary binding-specific substructure comparison and sequence profile alignment. Bioinformatics 29:2588–2595. https://doi.org/10.1093/bioinformatics/btt447
55. Jones G, Willett P, Glen RC et al (1997) Development and validation of a genetic algorithm for flexible docking. J Mol Biol 267:727–748. https://doi.org/10.1006/jmbi.1996.0897
56. Queyriaux B, Simon F, Grandadam M et al (2008) Clinical burden of chikungunya virus infection. Lancet Infect Dis 8:2–3. https://doi.org/10.1016/S1473-3099(07)70294-3
57. Mohan A, Kiran DHN, Manohar IC, Kumar DP (2010) Epidemiology, clinical manifestations, and diagnosis of Chikungunya fever: lessons learned from the re-emerging epidemic. Indian J Dermatol 55:54–63. https://doi.org/10.4103/0019-5154.60355
58. Pelosi G (2010) Thiosemicarbazone metal complexes: from structure to activity. Open Crystallogr J 3:16–28. https://doi.org/10.2174/1874846501003020016
59. Netalkar PP, Netalkar SP, Revankar VK (2015) Transition metal complexes of thiosemicarbazone: synthesis, structures and invitro antimicrobial studies. Polyhedron 100:215–222. https://doi.org/10.1016/j.poly.2015.07.075
60. Mondelli M, Pavan F, de Souza PC et al (2013) Study of a series of cobalt(II) sulfonamide complexes: synthesis, spectroscopic characterization, and microbiological evaluation against M. tuberculosis. Crystal structure of [Co(sulfamethoxazole)2(H2O)2]·H2O. J Mol Struct 1036:180–187. https://doi.org/10.1016/j.molstruc.2012.09.064
61. Langsjoen RM, Auguste AJ, Rossi SL et al (2017) Host oxidative folding pathways offer novel anti-chikungunya virus drug targets with broad spectrum potential. Antiviral Res 143:246–251. https://doi.org/10.1016/j.antiviral.2017.04.014
62. Lin Y, Betts H, Keller S et al (2021) Recent developments of metal-based compounds against fungal pathogens. Chem Soc Rev 50:10346–10402. https://doi.org/10.1039/D0CS00945H
63. Frei A (2020) Metal complexes, an untapped source of antibiotic potential? Antibiotics 9:90. https://doi.org/10.3390/antibiotics9020090
64. Ndagi U, Mhlongo N, Soliman M (2017) Metal complexes in cancer therapy – an update from drug design perspective. Drug Des Devel Ther 11:599–616. https://doi.org/10.2147/DDDT.S119488
65. de Paiva REF, Marçal Neto A, Santos IA et al (2020) What is holding back the development of antiviral metallodrugs? A literature overview and implications for SARS-CoV-2 therapeutics and future viral outbreaks. Dalt Trans 49:16004–16033. https://doi.org/10.1039/D0DT02478C
66. Chang EL, Simmers C, Knight DA (2010) Cobalt complexes as antiviral and antibacterial agents. Pharmaceuticals 3:1711–1728. https://doi.org/10.3390/ph3061711
67. Asbell P, Epstein SP, Wallace JA et al (1998) Efficacy of cobalt chelates in the rabbit eye model for epithelial herpetic keratitis. Cornea 17:550–557. https://doi.org/10.1097/00003226-199809000-00014
68. Schwartz JA, Lium EK, Silverstein SJ (2001) Herpes simplex virus type 1 entry is inhibited by the cobalt chelate complex CTC-96. J Virol 75:4117–4128. https://doi.org/10.1128/JVI.75.9.4117-4128.2001
69. Epstein SP, Pashinsky YY, Gershon D et al (2006) Efficacy of topical cobalt chelate CTC-96 against adenovirus in a cell culture model and against adenovirus keratoconjunctivitis in a rabbit model. BMC Ophthalmol 6:22. https://doi.org/10.1186/1471-2415-6-22
70. Louie AY, Meade TJ (1998) A cobalt complex that selectively disrupts the structure and function of zinc fingers. Proc Natl Acad Sci 95:6663–6668. https://doi.org/10.1073/pnas.95.12.6663
71. Cígler P, Kožíšek M, Řezáčová P et al (2005) From nonpeptide toward noncarbon protease inhibitors: metallacarboranes as specific and potent inhibitors of HIV protease. Proc Natl Acad Sci 102:15394–15399. https://doi.org/10.1073/pnas.0507577102
72. Řezáčová P, Pokorná J, Brynda J et al (2009) Design of HIV protease inhibitors based on inorganic polyhedral metallacarboranes. J Med Chem 52:7132–7141. https://doi.org/10.1021/jm9011388
73. Kirin VP, Demkin AG, Smolentsev AI et al (2016) Cobalt(III) complexes with biguanide derivatives: Synthesis, structures, and antiviral activity. Russ J Coord Chem Khimiya 42:260–266. https://doi.org/10.1134/S1070328416040023
74. Assunção-Miranda I, Cruz-Oliveira C, Neris RLS et al (2016) Inactivation of Dengue and Yellow Fever viruses by heme, cobalt-protoporphyrin IX and tin-protoporphyrin IX. J Appl Microbiol 120:790–804. https://doi.org/10.1111/jam.13038
75. Kaur P, Chu JJH (2013) Chikungunya virus: an update on antiviral development and challenges. Drug Discov Today 18:969–983. https://doi.org/10.1016/j.drudis.2013.05.002
76. Paeshuyse J, Dallmeier K, Neyts J (2011) Ribavirin for the treatment of chronic hepatitis C virus infection: a review of the proposed mechanisms of action. Curr Opin Virol 1:590–598. https://doi.org/10.1016/j.coviro.2011.10.030
77. Gallegos KM, Drusano GL, D'Argenio DZ, Brown AN (2016) Chikungunya virus. In vitro response to combination therapy with ribavirin and interferon alfa 2a. J Infect Dis 214:1192–1197. https://doi.org/10.1093/infdis/jiw358
78. Briolant S, Garin D, Scaramozzino N et al (2004) In vitro inhibition of Chikungunya and Semliki Forest viruses replication by antiviral compounds: synergistic effect of interferon-?? and ribavirin combination. Antiviral Res 61:111–117. https://doi.org/10.1016/j.antiviral.2003.09.005
79. Chen CH, Sigman DS (1986) Nuclease activity of 1,10-phenanthroline-copper: sequence-specific targeting. Proc Natl Acad Sci USA 83:7147–7151
80. Nakahata DH, de Paiva REF, Lustri WR et al (2018) Sulfonamide-containing copper(II) metallonucleases: correlations with in vitro antimycobacterial and antiproliferative activities. J Inorg Biochem 187:85–96. https://doi.org/10.1016/j.jinorgbio.2018.07.011
81. Molphy Z, Montagner D, Bhat SS et al (2018) A phosphate-targeted dinuclear Cu(II) complex combining major groove binding and oxidative DNA cleavage. Nucleic Acids Res 46:9918–9931. https://doi.org/10.1093/nar/gky806
82. Wada Y, Orba Y, Sasaki M et al (2017) Discovery of a novel antiviral agent targeting the nonstructural protein 4 (nsP4) of chikungunya virus. Virology 505:102–112. https://doi.org/10.1016/j.virol.2017.02.014
83. Oo A, Hassandarvish P, Chin SP et al (2016) In silico study on anti-Chikungunya virus activity of hesperetin. PeerJ 4:e2602. https://doi.org/10.7717/peerj.2602

84. Delang L, Segura Guerrero N, Tas A et al (2014) Mutations in the chikungunya virus non-structural proteins cause resistance to favipiravir (T-705), a broad-spectrum antiviral. J Antimicrob Chemother 69:2770–2784. https://doi.org/10.1093/jac/dku209
85. Daina A, Michielin O, Zoete V (2017) SwissADME: a free web tool to evaluate pharmacokinetics, drug-likeness and medicinal chemistry friendliness of small molecules. Sci Rep 7:42717. https://doi.org/10.1038/srep42717
86. Zhang Y, Rodionov DA, Gelfand MS, Gladyshev VN (2009) Comparative genomic analyses of nickel, cobalt and vitamin B12 utilization. BMC Genomics 10:78. https://doi.org/10.1186/1471-2164-10-78
87. Guan L, Yang H, Cai Y et al (2019) ADMET-score—a comprehensive scoring function for evaluation of chemical drug-likeness. Medchemcomm 10:148–157. https://doi.org/10.1039/C8MD00472B